

Electromagnetic Force Simulations on a Reaction Sphere for Satellite Attitude Control

L. Rossini^{*,1}, E. Onillon¹, O. Chételat¹, and C. Allegranza²

¹Swiss Center for Electronics and Microtechnology, Switzerland, ²ESA/ESTEC, The Netherlands.

*Corresponding author: CH-2002 Neuchâtel, Switzerland, leopoldo.rossini@csem.ch.

Abstract: In the frame of an ESA project, CSEM in collaboration with other partners has developed an innovative Attitude Orbit Control System concept that relies on a Reaction Sphere. We propose to use one unique magnetic bearing Reaction Sphere whose spin axis and angular velocity can be positioned by dedicated control. The design is based on a 3-D permanent magnet motor obtained with a multi pole rotor and a stator having 20 poles. The concept is protected under the patent WO 2007/113666 A2. We have manufactured a test platform and we have demonstrated some of the postulated characteristics of the Reaction Sphere concept. Finally, we have performed finite element simulations to verify the accuracy of the measurements on the test bench. Simulations results are in close agreement with the experimental results on the test platform.

Keywords: Reaction Sphere, attitude control system, spherical motor.

1. Introduction

Three reaction wheels appropriately arranged inside the spacecraft are normally employed as very accurate attitude control system (ACS), where the orientation of the satellite can be changed by accelerating the appropriate wheel [1]. However, in practice, four wheels are common because of optimization and redundancy purposes.

We proposed to use one unique Reaction Sphere held in position by magnetic levitation and accelerated about any rotation axis by a 3D motor [3]. The torque required for this acceleration is exported to the satellite and is used to change the satellite attitude. An ACS based on a Reaction Sphere would be smaller and lighter than today commonly employed systems and related costs are expected to be lower as well. Furthermore, the magnetic bearing Reaction Sphere is expected to reduce micro vibration contributions due to the absence of ball bearings and lubricants. Finally, the possibility

of using the Reaction Sphere as a 6 degree-of-freedom active vibration damper is an attractive feature of this concept.

The Reaction Sphere is based on a 3-D permanent magnet motor obtained with a multi pole rotor and a stator having 20 poles, each corresponding to one vertex of the dodecahedron.

In order to validate the Reaction Sphere concept as well as to assess its performances, some preliminary tests have been performed and several others are scheduled. The Reaction Sphere test bench used for the preliminary test is reported in section 3. We have measured the vertical force applied on the rotor for different rotor orientations and for a given current vector. The linearity between forces and torques has been confirmed by measurements. Furthermore, we have performed finite element simulations on the reaction Sphere model and we have measured forces and torques in a framework closed to the test bench setup. Finite element simulations are presented in section 4 and the results are reported in section 5 of this document.

2. Reaction Sphere Concept

2.1 Rotor Analysis

A three dimensional permanent magnet motor is obtained with a multi pole rotor. In order to maintain as much symmetry as possible, the number of regularly distributed poles on the rotor follows a cubic distribution as reported in Figure 1. The spherical rotor is composed by height quarters, each of them being either a north pole if $xyz > 0$ or a south pole otherwise (x , y , and z are the coordinates of a given point of the sphere). Contrary to the inductive or reluctance concepts, the permanent magnet synchronous motor presents the advantage of its linearity (current to force/torque) [4]. As consequence, the bearing and motor functions can be decoupled, easing the design and the development of a pure analytic model of the system. Torque and force productions are also decoupled. All losses

associated with the rotor of the induction motor are absent in this design and there is virtually no eddy current induced in the rotor.

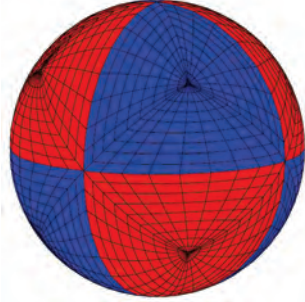


Figure 1. 8-pole permanent magnet rotor.

2.2 Stator Analysis

The reaction Sphere rotor can be controlled without discontinuities using 8-polar rotating fields. A 20-pole stator can produce an 8-polar rotating field in a symmetric manner since five cubes can share the vertices of the dodecahedron. Therefore, the stator has 20 poles, each corresponding to one vertex of the dodecahedron as depicted in Figure 2.



Figure 2. 20-pole stator.

3. Test Bench Demonstrator

The Reaction Sphere test bench setup is presented in Figure 3. For test purposes, the rotor is centered inside the stator with a rigid guiding axis along the gravity direction and it is free to rotate about it. Notice that the current physical axis of rotation does not have any specific symmetry that could in any case simplify the scenario, both from mechanical and magnetic perspectives. The stator is composed by a plastic spherical shell. The vertical force on the rotor is measured with a load cell.

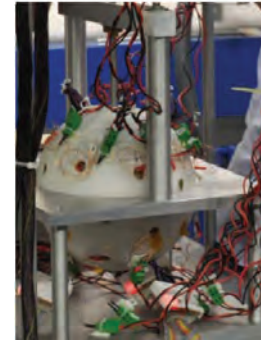


Figure 3. Test bench demonstrator.

4. Finite Element Simulations

4.1 Model Description

The schematic geometry for the magnetostatic finite element simulations without currents is presented in Figure 4. We have considered an ideal iron with linear B-H relationship and relative permeability equal to 4000. The magnets are implemented using a second quadrant demagnetization curve described by unitary relative permeability and parametric remanence following the 3-2 real spherical harmonic. In Cartesian coordinates, the latter gives:

$$\mathbf{B}_r = 3 \cdot B_{r0} \cdot \frac{xyz}{(x^2 + y^2 + z^2)^2} \cdot (x\hat{i} + y\hat{j} + z\hat{k})$$

The norm of the magnetic remanence vector will be specified by varying the parameter B_{r0} at the pole.

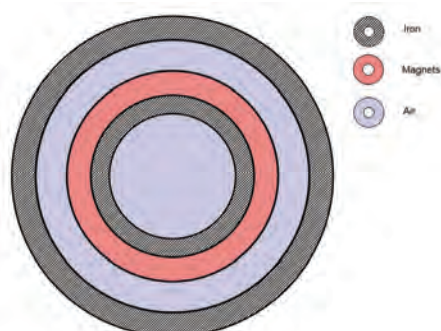


Figure 4. Schematic model geometry for finite element simulations. Coils and infinite elements are omitted in this figure. The diagram is not in scale.

Then, simulations with currents are obtained by adjusting the copper coils as presented in Figure 5.



Figure 5. Model geometry for finite element simulations showing coil distribution around the rotor.

4.2 Governing Equations

The equations governing the magnetic field inside all the domains of Figure 4 are essentially based on the magnetostatic analysis. The magnetic field can be derived by taking the gradient of the magnetic vector potential \mathbf{A} , which results by solving the Poisson's equation [2]

$$\nabla^2 \mathbf{A} = -\mu \mathbf{J}^e - \nabla \times \mathbf{B}_r$$

where \mathbf{J}^e is the external current density flowing in the coils, \mathbf{B}_r the magnet remanence, and μ the magnetic permeability.

5. Results

The radial magnetic flux density and the magnetic flux density at the rotor surface for a Reaction Sphere model with plastic stator are presented in Figure 6. In this figure, some parametric circular paths have been defined for radial magnetic flux density evaluation and reported in the image in magenta. In the figure, c1_5 is the lower path located at 5 mm from the rotor surface and c4_10 is the upper path located at 10 mm from the rotor surface. For illustration, the radial flux density about c2_5 and c2_10 is presented in Figure 7 for a Reaction Sphere setup

with plastic stator and magnetic remanence equal to 1.40 T.

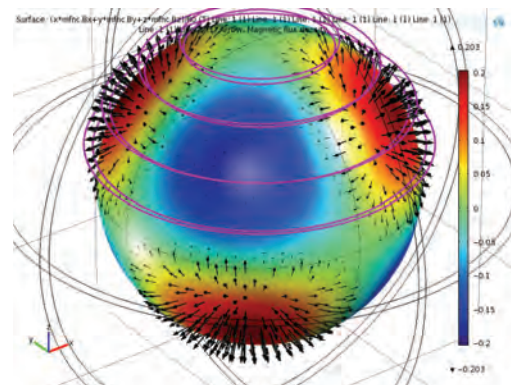


Figure 6. Radial magnetic flux density at the rotor surface (surface plot) and magnetic flux density (arrow plot). Reaction Sphere with plastic stator. Br=1.40 T. Circular paths for flux density evaluation represented in magenta.

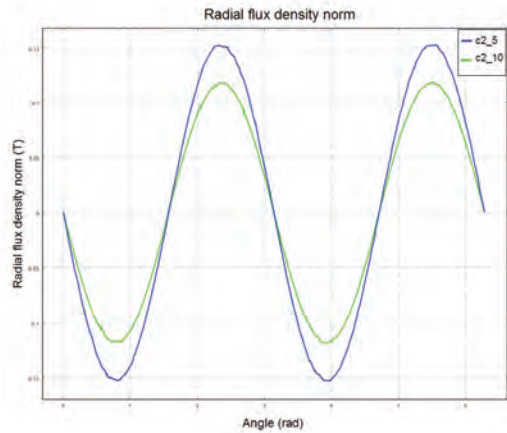


Figure 7. Radial flux density about the circular paths c2_5 and c2_10. Reaction Sphere without iron stator. Br=1.40 T.

For the simulations with current, the rotor orientation has been adjusted so as to match the one of the test bench setup. The radial magnetic flux density at the rotor surface (surface plot), the magnetic flux density at the rotor surface (arrow plot), and the current density in the coils (arrow plot) for a Reaction Sphere model with plastic stator is presented Figure 8. The vertical force is computed by integrating the Lorentz force on each of the twenty coils and summing up each contribution to obtain the net force. A summary of the computed and measured forces

for a given current vector varying its intensity is reported in Figure 9.

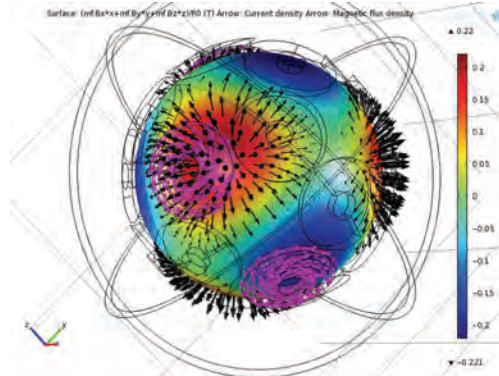


Figure 8. Radial magnetic flux density at the rotor surface (surface plot), magnetic flux density (arrow plot), and current density in the coils (arrow plot). Reaction Sphere with plastic stator. $B_r=1.4$ T.

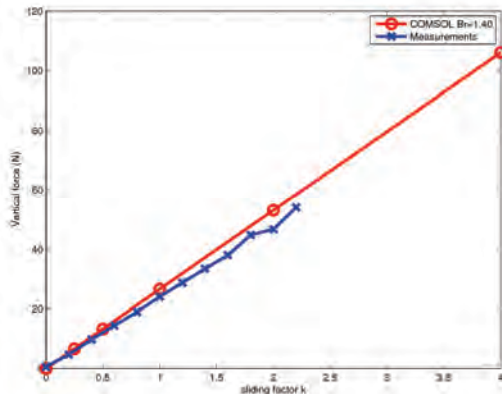


Figure 9. Computed forces using COMSOL and measurements on the test bench.

6. Conclusions

A Reaction Sphere prototype has been manufactured based on a synchronous motor concept. The Reaction Sphere is based on an eight-pole permanent magnet rotor and a 20-pole stator.

Preliminary tests to validate the Reaction Sphere model as well as its performances have been performed and several others are scheduled. We have measured the vertical force acting on the rotor for a given orientation and various current vectors demonstrating the linearity of the system.

Finally, we carried out several simulations using COMSOL. First, we simulated a

magnetostatic model without currents where the magnetic flux density of the Reaction Sphere rotor is computed with a plastic stator. Then, we added the coils to the model and we computed the vertical force by considering the same setup as in test bench used for the measurements. The COMSOL model turned out to be a powerful predictor for the forces as the computed values are in good agreement with the measurements.

7. References

1. Sidi, M. J., Spacecraft Dynamics and Control: A Practical Engineering Approach. Cambridge University Press. (1997)
2. Furlani, E., Permanent magnet and electromechanical devices. Academic Press. (2001).
3. Onillon, E., Chételat, O., Rossini, L., Lisowski, L., Droz, S., and Moerschell, J. Reaction sphere for attitude control. Proc. 13th European Space Mechanisms and Tribology Symposium 2009 (ESMATS 2009).
4. Jufer, M. Traité d'Electricité, volume IX, Electromécanique, Presses Polytechniques Romandes.